

Transition Metal(II)–Salen and –Salophen Macrocyclic Complexes for Rotaxane Formation: Syntheses and Crystal Structures

Mamiko Narita,^[a] Il Yoon,^[a] Masaru Aoyagi,^[a] Midori Goto,^[a] Toshimi Shimizu,^[a] and Masumi Asakawa*^[a]

Dedicated to Professor J. Fraser Stoddart on the occasion of his 65th birthday

Keywords: Rotaxanes / Ring opening / Ring closing / Transition metals / Porphyrinoids

We used a “threading-followed-by-shrinking” approach to prepare [2]rotaxanes possessing nickel(II)–salen and –salophen moieties. Reactions of macrocycles incorporating salen and salophen moieties with secondary dialkylammonium salts, followed by the addition of aqueous sodium sulfate, afforded the corresponding pseudorotaxanes; subsequent addition of nickel acetate shrank the effective size of the macrocycles to give the respective [2]rotaxanes. We obtained a [2]rotaxane possessing a salen unit in remarkably high yields – even in a polar solvent – indicating that the “threading-followed-by-shrinking” and “salen-ring-opening-and-closing” approaches occurred together. In addition,

we expanded the “threading-followed-by-shrinking” approach to prepare a [2]rotaxane and a bis[2]rotaxane comprising two palladium(II)–salophen moieties linked in a bis-macrocycle and one and two secondary dialkylammonium salts, respectively. Furthermore, we prepared a tetraphenylporphyrin rhodium(III) chloride [Rh(TPP)Cl]-stoppered [2]rotaxane comprising a palladium(II)–salophen macrocycle and a pyridyl-terminated thread-like ion coordinated to the rhodium(III) center, which has potential as a next-generation molecular machine exhibiting catalytic function.

(© Wiley-VCH Verlag GmbH & Co. KGaA, 69451 Weinheim, Germany, 2007)

Introduction

Interest in functionalized rotaxanes and their future potential as molecular machines in nanotechnology has increased in recent years.^[1] Many template-directed methods for the preparation of rotaxanes have appeared in the literature; they generally involve clipping,^[2] threading followed by stoppering,^[3] and slipping^[4] approaches. Functionalized rotaxanes can be immobilized onto solid surfaces through the use of self-assembled monolayers or Langmuir–Blodgett techniques.^[5] We demonstrated – through molecularly resolved scanning tunneling microscopy (STM) images – that porphyrin and phthalocyanine derivatives self-assemble

into ordered monolayer arrays on solid substrates.^[6] Furthermore, we synthesized porphyrin-stoppered rotaxanes, explicitly pseudorotaxanes bound to the metal centers of metalloporphyrins through axial coordination, which suggest that such organic molecules can be immobilized onto two-dimensional arrays of metalloporphyrins on a solid substrate.^[6a,6b,6d] Transition metals are often incorporated as templating or assembling centers for the formation of rotaxanes.^[7] Previously, we demonstrated the synthesis of a [2]rotaxane incorporating a palladium(II)–salophen [*N,N'*-*o*-phenylenebis(salicylideneiminato) dianion] moiety by using a “threading-followed-by-shrinking” approach (Figure 1a) that involves threading a rod-like unit through a macrocycle and then shrinking the free space within the macrocycle through coordination of its salophen moiety to palladium metal; the rotaxane formation in this system occurs in a nonpolar solvent (dichloromethane) when a sodium(I)-complexed macrocycle possessing a salophen unit is used.^[8] Furthermore, we reported the synthesis of monomeric and dimeric macrocycles incorporating salen [*N,N'*-ethylenebis(salicylideneiminato) dianion] moieties and a [2]-rotaxane formed by using a “ring-opening-and-closing” approach (Figure 1b) through the cleavage and formation of imino bonds of a salen moiety; the self-assembly of this macrocycle in the presence of a dumbbell-shaped rod-like component, followed by the addition of nickel acetate, af-

[a] Nanoarchitectonics Research Center, National Institute of Advanced Industrial Science and Technology (AIST), Tsukuba Central 5, 1-1-1 Higashi, Tsukuba Ibaraki 305-8565, Japan
Fax: +81-29-861-4679

E-mail: masumi-asakawa@aist.go.jp

[‡] Current address: Toyota Central R&D Labs., Inc., 41-1, Aza Yokomichi, Oaza Nagakute, Nagakute-cho, Aichi-gun, Aichi-Ken 480-1192, Japan

[‡‡] Current address: California NanoSystems Institute and Department of Chemistry and Biochemistry, University of California, Los Angeles, 405 Hilgard Avenue, Los Angeles, California 90095, USA

Supporting information for this article is available on the WWW under <http://www.eurjic.org> or from the author.

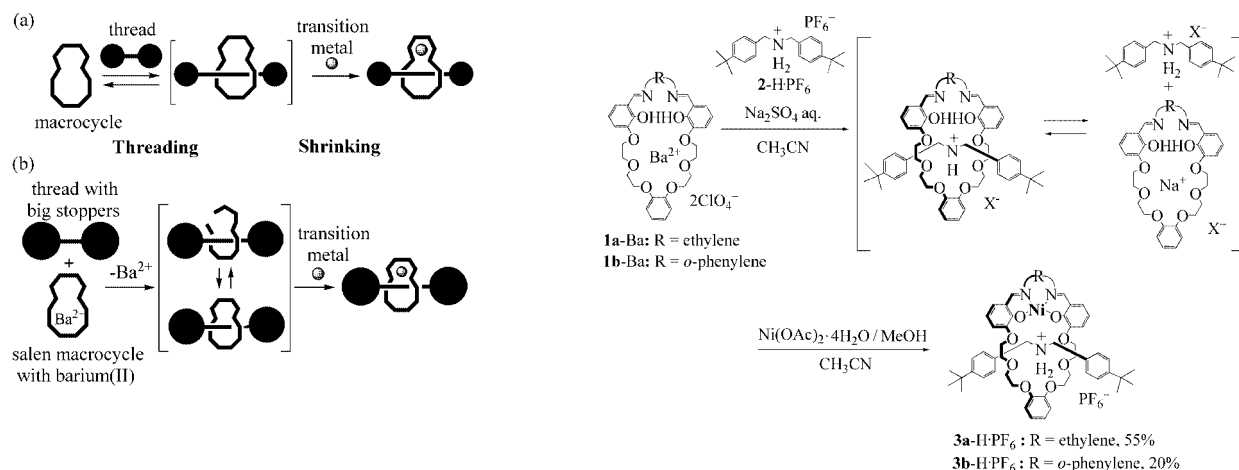
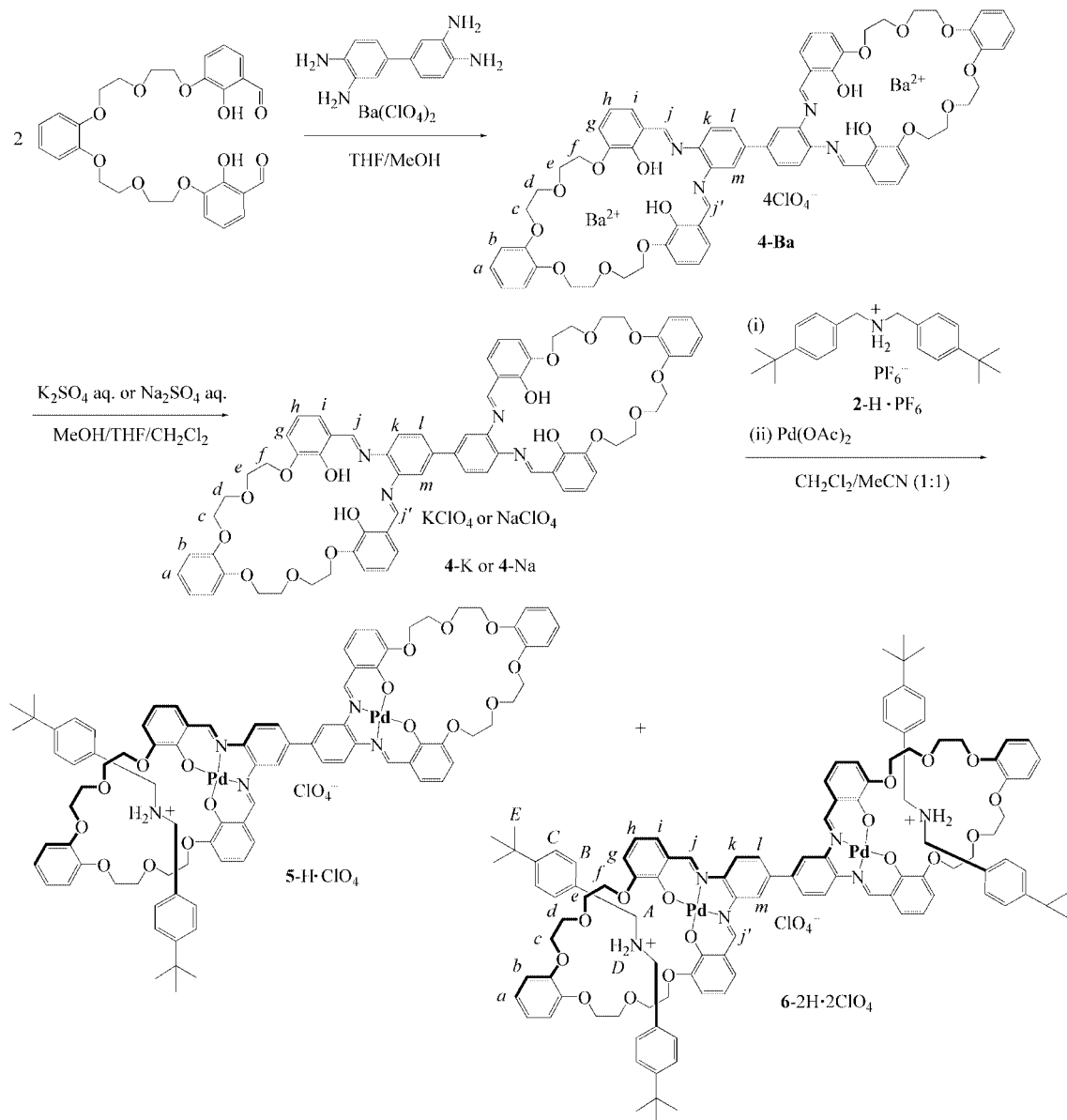


Figure 1. (a) “Threading-followed-by-shrinking” and (b) “ring-opening-and-closing” approaches toward [2]rotaxanes.

Scheme 1. Syntheses of [2]rotaxanes **3a-H-PF₆** and **3b-H-PF₆**.



Scheme 2. Syntheses of macrocycles **4-Ba**, **4-K**, **4-Na**, and rotaxanes **5-H-ClO₄** and **6-2H·2ClO₄**.

forded, after counterion exchange, a [2]rotaxane that was stabilized through coordination of the Ni ion to the macrocyclic salen moiety.^[9]

In this paper, we describe a different synthetic system in which we combined both “threading-followed-by-shrinking”^[8] and “ring-opening-and-closing”^[9] approaches – and note the remarkably higher yield for the synthesis of a salen-based rotaxane relative to that of our previous approach^[8] – for the formation of [2]rotaxanes **3a/b**·H·PF₆ (Scheme 1) from a precursor macrocycle [a barium(II)-complexed macrocycle possessing either a salen or salophen unit], a transition metal [nickel(II)], and a polar solvent (a mixture of water, methanol, and acetonitrile). Furthermore, we expanded the “threading-followed-by-shrinking” approach (Figure 2) to afford [2]rotaxane **5**·H·ClO₄ and bis-[2]rotaxane **6**·2H·2ClO₄, which features two palladium(II)–salophen moieties linked in a bismacrocycle (Scheme 2). The transition metal(II)–salen or –salophen moiety, which behaves as the shrinking center, might also be of use for applications in areas related to, for example, metallocatalysis,^[10] nonlinear optical response,^[11] and electron transfer^[12] when incorporated into rotaxane structures. In addition, we synthesized Rh(TPP)Cl-stoppered rotaxane **8**·H·Rh(TPP)Cl·ClO₄ (TPP = tetraphenylporphyrin;

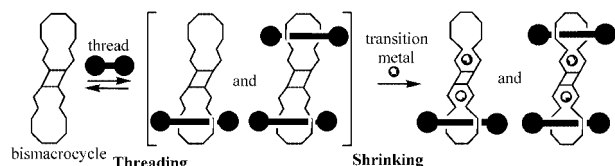
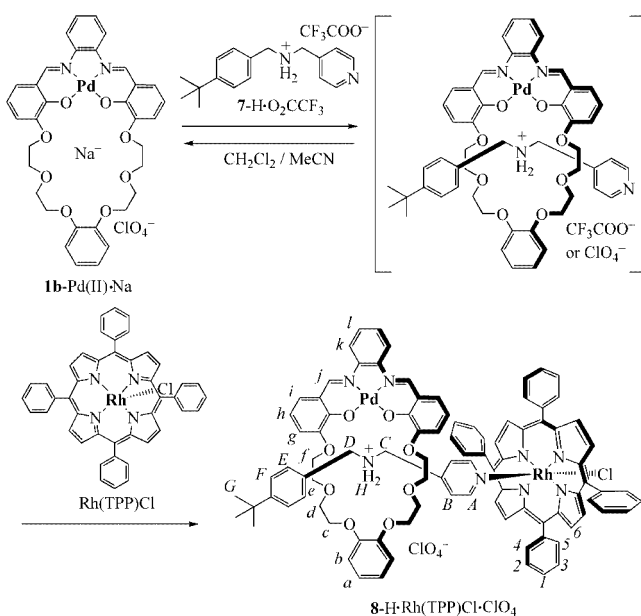


Figure 2. Graphical representation of the [2]rotaxane and bis[2]rotaxane when using the bismacrocycle and the “threading-followed-by-shrinking” approach.



Scheme 3. Synthesis of tetraphenylporphyrin-stoppered [2]rotaxane **8**·H·Rh(TPP)Cl·ClO₄.

Scheme 3) by combining sequential “threading-followed-by-shrinking” and end-capping approaches, the latter through axial coordination of a pyridyl unit in the thread-like component and the rhodium(III) metal center. Such rotaxanes may allow the construction of catalytically active molecular machines on solid surfaces. We characterized rotaxanes **3a/b**·H·PF₆, **5**·H·ClO₄, **6**·2H·2ClO₄, and **8**·H·Rh(TPP)Cl·ClO₄ by using NMR and IR spectroscopy, mass spectrometry, elemental analysis, and X-ray crystallography (see the Supporting Information).

Results and Discussion

As thread-like moieties, we used two types of the secondary dialkylammonium salt: **2**·H·PF₆,^[4c] which contains two terminal *t*Bu groups, and **7**·H·O₂CCF₃,^[13] which contains one *t*Bu group and one pyridyl unit as its termini. For the shrinking centers, we incorporated a salen moiety into macrocycle **1a**^[9] and salophen moieties into macrocycle **1b**^[2d] and bismacrocycle **4** (with each of these macrocycles prepared as a Ba complex). For end-capping, we used the rhodium(III) metal center of Rh(TPP)Cl. The reaction of **1a/b**·Ba and **2**·H·PF₆, followed by the addition of aqueous sodium sulfate, afforded the corresponding intermediate pseudorotaxanes, which could form free of macrocyclic and dumbbell components; the subsequent addition of nickel(II) acetate afforded [2]rotaxanes **3a/b**·H·PF₆ in yields of 55 and 20%, respectively (Scheme 1). The yield of rotaxane **3a**·H·PF₆, which incorporates the salen moiety, was remarkably high when considering that the use of polar solvents, which disrupt hydrogen bonding, was necessary because of the poor solubility of nickel(II) acetate in nonpolar solvents. Previously, we reported evidence for the “ring-opening-and-closing” approach occurring during the synthesis of a [2]rotaxane incorporating a salen moiety.^[9] We believe that the unexpectedly high yield of **3a**·H·PF₆ relative to that of **3b**·H·PF₆ may be attributed to the different environments experienced by the salen and salophen moieties during their respective “ring-opening-and-closing” processes, which occurred through reactions at their imine bonds. The relatively low yield in the synthesis of **3b**·H·PF₆ may have arisen from the fact that ring opening and closing are very slow in the macrocycle incorporating the salophen moiety. In the case of salen rotaxane **3a**·H·PF₆, both “threading-followed-by-shrinking” and “ring-opening-and-closing” processes occurred together, whereas salophen rotaxane **3b**·H·PF₆ formed only through the “threading-followed-by-shrinking” process.

For the synthesis of an extended system, we used the “threading-followed-by-shrinking” approach^[8] with bismacrocycle **4** possessing two macrocycle units linked through two salophen moieties (Figure 2). The reaction of two dialdehyde derivatives and 3,3'-diaminobenzidine afforded the barium(II)-complexed bismacrocycle possessing linked salophen moieties **4**·Ba (Scheme 2). The addition of aqueous potassium sulfate or aqueous sodium sulfate removed the coordinated barium(II) ions as precipitated

BaSO₄ to afford **4-K** or **4-Na**, respectively. The self-assembly of **4-K** or **4-Na** with **2-H**·PF₆, followed by the addition of palladium(II) acetate and counterion exchange, afforded a mixture of [2]rotaxane **5-H**·ClO₄ (i.e. possessing one thread-like moiety; 3% yield) and bis[2]rotaxane **6-2H**·2ClO₄ (i.e. possessing two thread-like moieties; 20% yield).

Toward our goal of immobilizing catalytically active rotaxanes as molecular machines on solid substrates, we synthesized the Rh(TPP)Cl-stoppered [2]rotaxane **8-H**·Rh(TPP)Cl·ClO₄. The reaction of **1b**·Pd^{II}·Na and 7-H·O₂CCF₃, followed by the addition of Rh(TPP)Cl and counterion exchange, afforded the Rh(TPP)Cl-stoppered [2]rotaxane **8-H**·Rh(TPP)Cl·ClO₄ in 40% yield (Scheme 3). The yield of this [2]rotaxane is lower than the one we achieved previously (75%)^[6b] when using dibenzo[24]-crown-8 as the macrocycle, possibly because of an increased steric clash between the larger salophen-containing macrocycle and the Rh(TPP)Cl unit or because of relatively weaker interactions between the components of this pseudorotaxane.

Figure 3 displays representative ¹H NMR spectra of [2]rotaxane **3a-H**·PF₆, the salen-incorporating macrocycle bound with nickel(II) [**1a**·Ni^{II}·Na],^[9] and thread-like salt **2-H**·PF₆. The ¹H NMR spectrum of **3a-H**·PF₆ (Figure 3c), together with its 2D ROESY and COSY NMR spectra (see Supporting Information) provides evidence for the successful formation of the [2]rotaxane. The signal of the CH₂N⁺ protons (*A*) in the rotaxane has shifted downfield significantly relative to that in the free thread (Figure 3a) as a result of the formation of [C–H···O] hydrogen bonds^[14] (Figure 6). In addition, these protons (*A*) resonate as a triplet in the rotaxane (Figure 3c), whereas they appear as a singlet in the free thread (Figure 3a), which might be a result of the reduced exchange rates of the ammonium protons in the rotaxane structure owing to the hydrogen bonds.

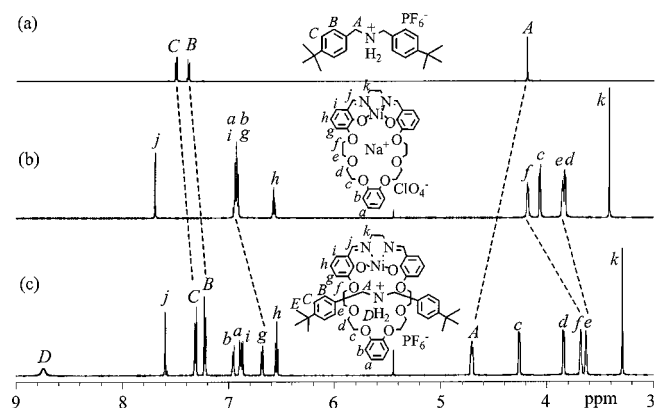


Figure 3. ¹H NMR spectra (600 MHz, CD₃CN, 25 °C) of (a) **2-H**·PF₆, (b) **1a**·Ni^{II}·Na(I), and (c) **3a**·H·PF₆.

In contrast, two of the signals for the ether CH₂O protons (*e* and *f*; Figure 3c) in the Ni^{II}-bound macrocycle of the rotaxane have shifted upfield relative to their location in the unthreaded Ni^{II}-complexed macrocycle (Figure 3b); we attribute this phenomenon to shielding by the aromatic

units in the thread in bent conformations of the components (Figure 6). In addition, the signals of the protons of the aromatic groups in the salen moiety (*g*; Figure 3c) as well as in the thread (*B* and *C*; Figure 3c) have shifted upfield relative to their locations in the corresponding free components probably as a result of π – π stacking interactions.^[15] As indicated in Figure 4, the ¹H NMR spectrum of [2]rotaxane **3b**·H·PF₆ (Figure 4c) displays signals that are very similar to those observed for **3a**·H·PF₆, which provides good evidence of the successful formation of this rotaxane. Moreover, the ROESY NMR spectra (see Supporting Information) of both rotaxanes **3a/b**·H·PF₆ feature cross peaks between the signals of the protons of the ether units (*e* and *f*) in their respective macrocycles and the CH₂N⁺ units (*A*) in their thread-like moieties.

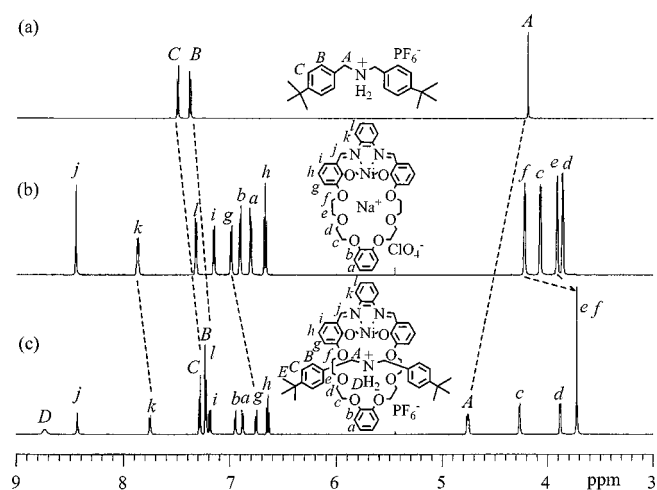


Figure 4. ¹H NMR spectra (600 MHz, CD₃CN, 25 °C) of (a) **2-H**·PF₆, (b) **1b**·Ni^{II}·Na(I), and (c) **3b**·H·PF₆.

Figure 5 displays representative ¹H NMR spectra of bis[2]rotaxane **6-2H**·2ClO₄, the salophen-incorporating bismacrocycle bound with palladium(II) [**4**·Pd^{II}·Na; for its synthesis, see the Supporting Information], and thread-like salt **2-H**·PF₆. Most of signals for the protons of bis[2]rotaxane **6-2H**·2ClO₄ (Figure 5c–e) are very similar to those observed for [2]rotaxanes **3a/b**·H·PF₆, which provides good evidence for the successful formation of this rotaxane and confirms its structure. At 25 °C (Figure 5c), the protons of the salophen and ether units in the bismacrocycle suggest that slow conformational changes occur on the ¹H NMR spectroscopic timescale, which results in broadening and splitting (*e*, *h*, and *j*) of the signals for a few protons of the bismacrocycle. The spectrum became much simpler when the signals for these protons coalesced at higher temperatures (Figure 5d, e). In addition, the ROESY NMR spectrum (see Supporting Information) of this bis[2]rotaxane features cross peaks between the signals of the protons of the ether unit (*c* and *d*) in the bismacrocycle component and aromatic protons (*B* and *C*) in its two thread-like moieties.

The ¹H NMR spectrum of the Rh(TPP)Cl-stoppered [2]rotaxane **8-H**·Rh(TPP)Cl·ClO₄ (see Supporting Information) displays signals that are very similar to those that

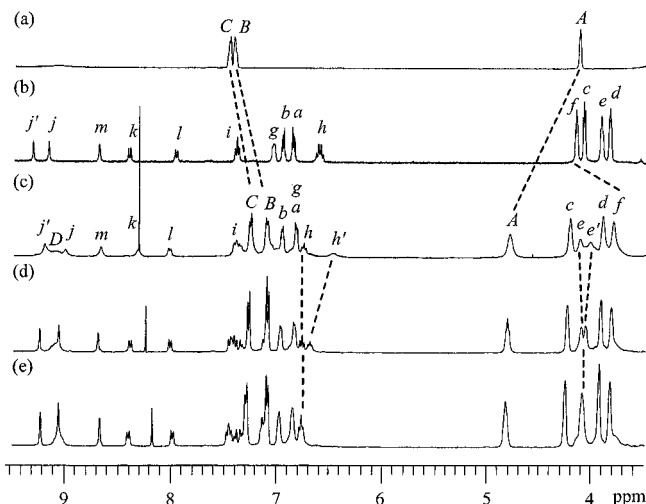


Figure 5. ^1H NMR spectra (400 MHz, $[\text{D}_6]\text{DMSO}$) of (a) $2\text{-H}\cdot\text{PF}_6$, (b) $4\text{-Pd}^{\text{II}}\cdot\text{Na}(\text{I})$, and $6\text{-2H}\cdot 2\text{ClO}_4$ recorded at temperatures of (c) 298 K, (d) 323 K, and (e) 353 K.

we observed previously.^[6a,6b,6d] In particular, the signal of the aromatic protons (*A*; Scheme 3) in the terminal pyridyl unit of the thread-like moiety is shifted upfield drastically relative to that in the free salt as a result of the shielding effect of the diamagnetic current of the porphyrin ring.^[16]

We obtained dark-brown-colored single crystals of $3\text{a}\text{-H}\cdot\text{PF}_6$ that were suitable for X-ray crystallographic analysis upon slow evaporation of a $\text{CH}_2\text{Cl}_2/\text{EtOAc}$ solution of the [2]rotaxane; $3\text{b}\text{-H}\cdot\text{PF}_6$ provided yellowish-brown-colored single crystals, also suitable for X-ray crystallographic analysis, upon vapor diffusion of diisopropyl ether into a CH_2Cl_2 solution of the [2]rotaxane. The crystal structures

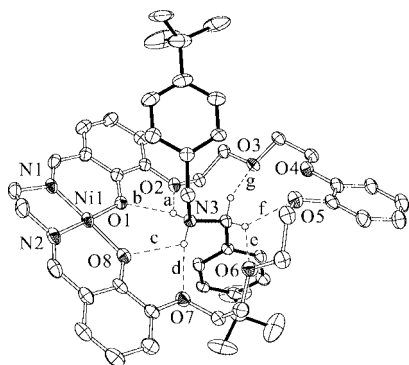


Figure 6. One molecular structure of $3\text{a}\text{-H}\cdot\text{PF}_6$ that indicates the intercomponent $[\text{N}^+\text{-H}\cdots\text{O}]$ and $[\text{C}\text{-H}\cdots\text{O}]$ hydrogen bonds. The other rotaxane molecule, the nonhydrogen-bonding hydrogen atoms, disordered carbon atoms, and the counter anion have been omitted for clarity. Hydrogen bonding geometries: $[\text{X}\cdots\text{O}]$, $[\text{H}\cdots\text{O}]$ distances [Å] and $[\text{X}\text{-H}\cdots\text{O}]$ angles [°] are (a) 3.067, 2.348, 136.8; (b) 2.840, 2.032, 148.6; (c) 2.737, 2.207, 117.1; (d) 2.892, 2.008, 166.8; (e) 3.264, 2.523, 134.0; (f) 3.429, 2.580, 147.6; (g) 3.185, 2.318, 149.9.

(Figures 6 and 7, respectively) confirm the proposed [2]rotaxane structures incorporating the nickel(II)–salen and –salophen moieties, respectively. Stabilization of these [2]rotaxanes is achieved through a combination of (1) $[\text{N}^+\text{-H}\cdots\text{O}]^{[17]}$ and $[\text{C}\text{-H}\cdots\text{O}]^{[17a,17c]}$ hydrogen bonds involving NH_2^+ centers, their adjacent CH_2 groups, and the oxygen atoms in the macrocycles and (2) $\pi\text{-}\pi$ stacking interactions^[17] between aromatic rings (see Supporting Information). The packing arrays of both $3\text{a/b}\text{-H}\cdot\text{PF}_6$ are stabilized by intra- and intermolecular $[\text{C}\text{-H}\cdots\pi]$ interactions.^[17b,17d] The $[\text{N}^+\text{-H}\cdots\text{O}]^{[17]}$ and $[\text{C}\text{-H}\cdots\text{O}]^{[17a,17c]}$ hydrogen bonding distances (2.737–3.498 Å) are comparable to those found in a related [2]rotaxane incorporating a palladium(II)–salophen,^[8] a nickel(II)–salen^[9] moiety, and other^[17] similar compounds. The nickel atom exists in a distorted square-planar array (see Supporting Information) that is very similar to the geometries we have observed previously for palladium atoms in related structures.^[8,12d]

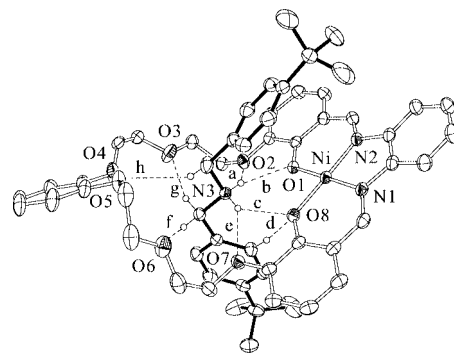


Figure 7. Molecular structure of $3\text{b}\text{-H}\cdot\text{PF}_6$ that indicates the intercomponent $[\text{N}^+\text{-H}\cdots\text{O}]$ and $[\text{C}\text{-H}\cdots\text{O}]$ hydrogen bonds. The nonhydrogen-bonding hydrogen atoms, disordered carbon atoms, and the counter anion have been omitted for clarity. Hydrogen bonding geometries: $[\text{X}\cdots\text{O}]$, $[\text{H}\cdots\text{O}]$ distances [Å] and $[\text{X}\text{-H}\cdots\text{O}]$ angles [°] are (a) 2.906, 2.148, 141.5; (b) 2.829, 2.074, 140.7; (c) 2.858, 2.127, 137.8; (d) 3.498, 2.572, 162.1; (e) 2.920, 2.141, 144.4; (f) 3.408, 2.545, 149.7; (g) 3.259, 2.329, 162.8; (h) 3.323, 2.575, 134.9.

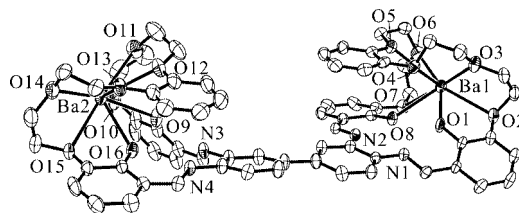


Figure 8. Molecular structure of 4-Ba . Perchlorate anions, solvent molecules, and hydrogen atoms have been omitted for clarity. Selected bond lengths [Å] and angles [°]: Ba1–O1 2.745(5), Ba1–O2 3.001(5), Ba1–O3 2.975(5), Ba1–O4 2.934(5), Ba1–O5 3.010(5), Ba1–O6 2.965(5), Ba1–O7 2.903(5), Ba1–O8 2.786(5), Ba2–O9 2.828(5), Ba2–O10 3.046(6), Ba2–O11 2.945(6), Ba2–O12 2.932(6), Ba2–O13 2.956(5), Ba2–O14 2.984(6), Ba2–O15 2.995(6), Ba2–O16 2.816(5); O1–Ba1–O6 156.66(15), O8–Ba1–O3 116.71(14), O7–Ba1–O3 171.01(15), O4–Ba1–O2 98.17(14), O6–Ba1–O2 147.28(14), O2–Ba1–O5 149.92(14), O16–Ba2–O11 122.12(17), O9–Ba2–O14 154.50(16), O12–Ba2–O15 119.58(17), O11–Ba2–O15 175.73(17), O13–Ba2–O10 152.92(16), O14–Ba2–O10 150.05(16).

We obtained orange-colored single crystals of **4-Ba** suitable for X-ray crystallographic analysis upon the slow evaporation of a $\text{CH}_2\text{Cl}_2/\text{THF}/\text{MeOH}$ solution of the Ba^{II} -coordinated bismacrocycle. The crystal structure (Figure 8) confirms that this bismacrocycle possesses two barium(II) ions; the two salophen macrocyclic units, which are attached through aromatic rings, are twisted at a dihedral angle of 14.8° . Each oligoether unit is folded completely to allow coordination of all of its oxygen atoms to the barium(II) ion.

Conclusions

We synthesized [2]rotaxanes **3a/3b-H-PF₆** that feature nickel(II)–salophen and –salen moieties, respectively. Both “ring-opening-and-closing” and “threading-followed-by-shrinking” processes occurred during the synthesis of the salen-based [2]rotaxane **3a-H-PF₆**, resulting in its remarkably higher yield than that of the salophen-based [2]rotaxane **3b-H-PF₆**, for which only a “threading-followed-by-shrinking” process occurs. During the formation of these [2]rotaxanes, the binding of nickel(II) ions to the salophen and salen moieties constitutes the shrinking event. Furthermore, we extended the synthetic system by using a “threading-followed-by-shrinking” approach to afford [2]rotaxane **5-H-ClO₄** and bis[2]rotaxane **6-2H-2ClO₄**, which both feature two palladium(II)–salophen moieties linked in a bismacrocycle. In addition, we synthesized the Rh(TPP)Cl-stoppered [2]rotaxane **8-H-Rh(TPP)Cl-ClO₄** from salophen-based macrocycle **1b-Pd^{II}-Na** by using a combination of “threading-followed-by-shrinking” and end-capping through axial coordination between the pyridyl unit of the thread-like cationic component and the rhodium(III) center. We believe that these approaches will be useful for the construction of multifunctional rotaxanes and for the development of molecular devices as new tools. Such rotaxanes possessing salen and salophen moieties have the potential to behave as catalytically active molecular machines on solid surfaces.

Experimental Section

General Information: Nickel(II) acetate tetrahydrate, 3,3'-diaminobenzidine, palladium(II) acetate, and tetracarbonyl-di- μ -chlororhodium(I) ($[\text{Rh}(\text{CO})_2\text{Cl}]_2$) were purchased from Aldrich. Sodium sulfate, potassium sulfate, and barium perchlorate were purchased from Wako Pure Chemical Industries. **1a-Ba**^[9] (Scheme 1), **1b-Ba**^[12d] (Scheme 1), **1a-Ni^{II}-Na**^[9], **1b-Pd^{II}-Na**^[12d] (Scheme 3), **2-H-PF₆**^[4c] (Scheme 1), **7-H-CF₃COO**^[13] (Scheme 3), and Rh(TPP)Cl^[6b] (Scheme 3) were all prepared according to literature procedures. Solvents were purchased from commercial sources. Each reaction was performed under an anhydrous nitrogen atmosphere. Thin-layer chromatography (TLC) was performed by using aluminum sheets precoated with silica gel 60F (Merck 5554). The plates were inspected under UV light and developed in I_2 vapor. Column chromatography was conducted by using Wakogel C-400HG (Wako Pure Chemical Industries). ¹H and ¹³C NMR spectra were recorded with a Bruker AVANCE 400 spectrometer (400 and 100 MHz for ¹H and ¹³C NMR, respectively). All 2D NMR spec-

trosopy experiments were recorded by using 1 K data points and 256 time increments in phase-sensitive mode and were processed in a $1\text{ K} \times 1\text{ K}$ matrix. The ROESY NMR spectroscopic experiment was performed with the use of a spin-lock mixing time of 200 ms and was processed using a forward linear prediction in the F1 dimension. Matrix-assisted laser-desorption/ionization time-of-flight mass spectrometry (MALDI-TOF MS) was performed with a Shimadzu Kratos Kompact-MALDI III with a 2,5-dihydroxybenzoic acid as the matrix. FAB mass spectra were recorded with an MS600H spectrometer. Infrared (IR) spectra were recorded by using a Jasco FTIR 620 spectrophotometer. Elemental analyses were performed with a CE Instruments EA1110. Gel permeation chromatography (GPC) separation was performed with an LC-918 (Japan Analytical Industry Co. Ltd.) equipped with JAIGL-1H and -2H columns; chloroform was used as the eluent.

Macrocycle Coordinated to Both Nickel(II) and Sodium(I), 1b-Ni^{II}-Na: A solution of sodium sulfate (2.00 g, 14.0 mmol) in water (20 mL) was added to a solution of **1b-Ba** (935 mg, 1.0 mmol) in MeCN (40 mL), and then the mixture was stirred at r.t. for 3 h. The reaction mixture was filtered to remove the precipitated barium sulfate. The filtrate was dried (anhydrous Na_2SO_4), the solvent was evaporated, and the residue was dried under high vacuum to yield **1b-Na** as an orange solid (801 mg, 95%). A solution of nickel(II) acetate tetrahydrate (274 mg, 1.1 mmol) in MeOH (12 mL) was added to a solution of **1b-Na** (616 mg, 0.73 mmol) in CH_2Cl_2 (40 mL), and then the mixture was stirred at r.t. for 2 h. The solvent was evaporated under reduced pressure. The residue was dissolved in a small amount of MeCN and purified by column chromatography (SiO_2 ; $\text{CH}_2\text{Cl}_2/\text{MeOH}$, 98:2). Fractions containing the product ($R_f = 0.42$ for **1b-Ni^{II}-Na**; $\text{CH}_2\text{Cl}_2/\text{MeOH}$, 9:1) were combined, and the solvent was evaporated under reduced pressure to afford **1b-Ni^{II}-Na** (454 mg, 80%) as a brown solid. M.p. $141\text{--}142^\circ\text{C}$. ¹H NMR (400 MHz, CD_3CN , 25°C): $\delta = 8.00$ (s, 2 H, *j*), 7.44 (br., 2 H, *k*), 6.89–6.86 (m, 2 H, *a*), 6.79–6.74 (m, 6 H, *b*, *i*, *l*), 6.61 (d, *J* = 7.8 Hz, 2 H, *g*), 6.40 (t, *J* = 7.8 Hz, 2 H, *h*), 4.13 (br., 4 H, *f*), 4.07 (br., 4 H, *c*), 3.86–3.85 (br., 8 H, *d/e*) ppm. ¹³C NMR (100 MHz, CD_3CN , 25°C): $\delta = 155.3$, 154.1, 148.4, 147.3, 141.9, 127.4, 125.5, 121.7, 119.7, 115.4, 115.1, 114.7, 68.9, 68.2, 67.8, 67.0 ppm. IR (KBr): $\tilde{\nu} = 3504$, 2920, 2874, 1707, 1610, 1543, 1503, 1450, 1254, 1202, 1100 (ClO_4^-), 936, 739 cm^{-1} . MS (MALDI-TOF): $m/z = 678$ (100) [$\text{M} + 1 - \text{ClO}_4$]⁺. $\text{C}_{34}\text{H}_{32}\text{ClN}_2\text{NaNiO}_{12}$ (777.77): calcd. C 52.51, H 4.15, N 3.60; found C 52.58, H 4.28, N 3.51.

3a/b-H-PF₆: A solution of Na_2SO_4 (101 mg, 0.71 mmol) in H_2O (2 mL) and MeCN (2 mL) was added to a solution of the relevant macrocycle–barium perchlorate complex (0.25 mmol; 222 mg for **1a-Ba**; 234 mg for **1b-Ba**) and **2-H-PF₆** (229 mg, 0.50 mmol) in MeCN (20 mL), and then the mixture was stirred for 2 h. A solution of $\text{Ni}(\text{OAc})_2 \cdot 4\text{H}_2\text{O}$ (63.3 mg, 0.25 mmol) in MeOH (2 mL) and MeCN (2 mL) was added to the reaction mixture, which was stirred for 12 h. The solution was filtered, and then the solvent was evaporated under reduced pressure. The residue was dissolved in a small amount of MeCN and purified by column chromatography (SiO_2 ; $\text{CH}_2\text{Cl}_2/\text{MeOH}$, 9:1). Fractions containing the product ($R_f = 0.37$ for **3a-H-PF₆**; $R_f = 0.33$ for **3b-H-PF₆**; $\text{CH}_2\text{Cl}_2/\text{MeOH}$, 9:1) were combined, and the solvent was evaporated under reduced pressure to afford the [2]rotaxanes as either a yellow-green (**3a-H-PF₆**; 146 mg, 55%) or dark-brown solid (**3b-H-PF₆**; 56 mg, 20%). Selected data for **3a-H-PF₆**: M.p. $145\text{--}147^\circ\text{C}$ (decomp.). ¹H NMR (600 MHz, CD_3CN , 25°C): $\delta = 8.74$ (br., 2 H, *D*), 7.60 (s, 2 H, *j*), 7.31 (d, *J* = 8.4 Hz, 4 H, *C*), 7.23 (d, *J* = 8.4 Hz, 4 H, *B*), 6.95 (m, 2 H, *b*), 6.90 (m, 2 H, *a*), 6.88 (d, *J* = 7.8 Hz, 2 H, *i*), 6.68 (d, *J* = 7.8 Hz, 2 H, *g*), 6.55 (t, *J* = 7.8 Hz, 2 H, *h*), 4.71 (t, *J* = 6.6 Hz, 4 H, *A*), 4.25 (m, 4 H, *c*), 3.85 (m, 4 H, *d*), 3.68 (m, 4 H, *f*), 3.63 (m,

4 H, *e*), 3.29 (s, 4 H, *k*), 1.22 (s, 18 H, *E*) ppm. ^{13}C NMR (150 MHz, CD_3CN , 25 °C): δ = 163.2, 152.7, 150.6, 147.9, 147.6, 130.2, 128.3, 124.8, 124.7, 120.5, 120.2, 114.8, 114.1, 111.9, 68.8, 68.3, 67.6, 67.1, 58.4, 50.4, 33.9, 30.3 ppm. IR (KBr): $\tilde{\nu}$ = 3436, 3094, 2958, 1629, 1607, 1549, 1504, 1450, 1304, 1228, 1132, 1089, 839 (PF_6^-), 741, 557 cm^{-1} . MS (FAB): m/z (%) = 916 (72) [$\text{M} - \text{PF}_6$] $^+$. $\text{C}_{52}\text{H}_{64}\text{F}_6\text{N}_3\text{NiO}_8\text{P}$ (1062.75): calcd. C 58.77, H 6.07, N 3.95; found C 59.07, H 6.27, N 3.61. Selected data for **3b-H**· PF_6 : M.p. 314–315 °C. ^1H NMR (600 MHz, CD_3CN , 25 °C): δ = 8.73 (br., 2 H, *D*), 8.44 (s, 2 H, *j*), 7.73 (m, 2 H, *k*), 7.28 (d, J = 8.4 Hz, 4 H, *C*), 7.24 (d, J = 8.4 Hz, 4 H, *B*), 7.21 (m, 2 H, *l*), 7.19 (d, J = 7.8 Hz, 2 H, *i*), 6.94 (m, 2 H, *b*), 6.89 (m, 2 H, *a*), 6.73 (d, J = 7.8 Hz, 2 H, *g*), 6.64 (t, J = 7.8 Hz, 2 H, *h*), 4.78 (t, J = 6.6 Hz, 4 H, *A*), 4.28 (m, 4 H, *c*), 3.88 (m, 4 H, *d*), 3.72 (s, 8 H, *elf*), 1.09 (s, 18 H, *E*) ppm. ^{13}C NMR (150 MHz, CD_3CN , 25 °C): δ = 156.9, 154.2, 150.9, 147.8, 147.5, 142.0, 130.1, 128.2, 127.9, 126.6, 124.6, 120.5, 120.3, 115.6, 115.5, 115.1, 111.9, 68.8, 68.0, 67.6, 67.0, 50.6, 33.7, 30.0 ppm. IR (KBr): $\tilde{\nu}$ = 3067, 2961, 1618, 1441, 1258, 1204, 1103, 840 (PF_6^-), 743, 556 cm^{-1} . MS (FAB): m/z (%) = 965 (90) [$\text{M} + 1 - \text{PF}_6$] $^+$. $\text{C}_{56}\text{H}_{64}\text{F}_6\text{N}_3\text{NiO}_8\text{P}$ (1110.79): calcd. C 60.55, H 5.81, N 3.78; found C 60.88, H 5.88, N 3.47.

4-Ba: A solution of the dialdehyde-functionalized crown ether derivative (526.5 mg, 1.0 mmol) and 3,3'-diaminobenzidine (107.2 mg, 0.5 mmol) in dry THF (20 mL) was added over 2 h to a solution of barium perchlorate (336.3 mg, 1.0 mmol) heated under reflux in dry MeOH (100 mL). The mixture was heated under reflux for an additional 24 h. During the reaction, an orange-colored solid precipitated out. This solid was filtered off and washed with CH_2Cl_2 to afford the barium perchlorate–bismacrocycle complex **4-Ba** as an orange solid (691 mg, 74%). M.p. 221–226 °C. ^1H NMR (400 MHz, CD_3CN , 25 °C): δ = 14.89–14.67 (m, 4 H, *OH*), 9.42 (br., 2 H, *j'*), 9.04 (br., 2 H, *j*), 8.02 (s, 2 H, *m*), 7.95–7.90 (m, 2 H, *k*), 7.74–7.69 (m, 2 H, *l*), 7.24 (m, 4 H, *i*), 7.08 (m, 4 H, *g*), 6.93–6.85 (m, 8 H, *a, b*), 6.61 (m, 4 H, *h*), 4.47 (m, 8 H, *f*), 3.97–3.82 (m, 24 H, *c–e*) ppm. IR (KBr): $\tilde{\nu}$ = 1080 (ClO_4^-) cm^{-1} . MS (FAB): m/z (%) = 1431 (10) [$\text{M} - \text{Ba} - 3\text{ClO}_4$] $^+$. $\text{C}_{68}\text{H}_{66}\text{Ba}_2\text{Cl}_4\text{N}_4\text{O}_{32} \cdot 3\text{H}_2\text{O}$ (1921.80): calcd. C 42.50, H 3.78, N 2.92; found C 42.23, H 3.92, N 2.69.

4-K and **4-Na**: A solution of potassium sulfate (1 g, 5.7 mmol) or sodium sulfate (0.81 g, 5.7 mmol) in H_2O (50 mL) was added to a solution of **4-Ba** (1.06 g, 0.57 mmol) in a solution of MeOH/THF/MeCN/Me₂CO (4:4:1:1, 200 mL), and then the mixture was stirred at r.t. for 3 h. The reaction mixture was filtered to remove the precipitated barium sulfate. The solvent was evaporated, and the residue was dried under high vacuum to yield **4-K** as an orange solid (684 mg, 90%) or **4-Na** as an orange solid (683 mg, 91%). Selected data for **4-K**: ^1H NMR (400 MHz, $[\text{D}_6]\text{DMSO}$, 25 °C): δ = 13.59–13.56 (m, 4 H, *OH*), 9.11–9.02 (m, 4 H, *j, j'*), 8.55 (s, 2 H, *m*), 7.99 (m, 2 H, *k*), 7.67 (m, 2 H, *l*), 7.29–7.26 (m, 4 H, *i*), 7.15–7.14 (m, 4 H, *g*), 6.98–6.91 (m, 8 H, *a, b*), 6.89–6.86 (m, 4 H, *h*), 4.17 (m, 8 H, *f*), 4.11 (m, 8 H, *c*), 3.86 (m, 8 H, *e*), 3.83–3.82 (m, 8 H, *d*) ppm. ^{13}C NMR (100 MHz, $[\text{D}_6]\text{DMSO}$, 25 °C): δ = 192.3, 192.2, 150.9, 150.8, 150.3, 148.1, 147.7, 147.6, 146.8, 146.3, 146.0, 143.9, 124.2, 121.8, 121.7, 120.8, 120.6, 118.7, 118.6, 118.0, 114.3, 113.7, 98.7, 54.3, 52.6, 48.0, 30.0 ppm. IR (KBr): $\tilde{\nu}$ = 1100 (ClO_4^-) cm^{-1} . MS (FAB): m/z (%) = 1233 (10) [$\text{M} - \text{ClO}_4$] $^+$.

4-Pd^{II}-Na: Solid palladium(II) acetate (384 mg, 1.71 mmol) was added to a CH_2Cl_2 /THF/MeOH (6:2:2, 200 mL) solution of **4-Na** (751 mg, 0.57 mmol), and then the mixture was stirred at r.t. for 2 h. The solvent was evaporated under reduced pressure. The residue was dissolved in a small amount of MeCN and purified by column chromatography (SiO_2 ; CH_2Cl_2 /MeOH, 98:2) to afford **4-**

Pd^{II}-Na (752 mg, 80%) as an orange solid. ^1H NMR (400 MHz, $[\text{D}_6]\text{DMSO}$, 25 °C): δ = 9.37 (s, 2 H, *j'*), 9.22 (s, 2 H, *j*), 8.74 (s, 2 H, *m*), 8.45 (d, J = 9 Hz, 2 H, *k*), 8.02 (d, J = 9 Hz, 2 H, *l*), 7.43 (m, 4 H, *i*), 7.08 (br., 4 H, *g*), 6.98 (m, 4 H, *b*), 6.91 (m, 4 H, *a*), 6.66 (m, 4 H, *h*), 4.21 (br., 8 H, *f*), 4.14 (br., 8 H, *c*), 3.97 (br., 8 H, *e*), 3.89 (br., 8 H, *d*) ppm. IR (KBr): $\tilde{\nu}$ = 3003, 2391, 1853, 1630, 1481, 1346, 1163, 1053 (ClO_4^-), 976 cm^{-1} . MS (MALDI-TOF): m/z (%) = 1428 (100) [$\text{M} + 1 - \text{Na} - 2\text{ClO}_4$] $^+$, 1548 (4) [$\text{M} - 1 - \text{ClO}_4$] $^+$.

5-H· ClO_4 and **6-2H**· 2ClO_4 : A solution of **2-H**· PF_6 (592 mg, 1.3 mmol) in MeCN (20 mL) was added to a solution of the bismacrocycle with potassium(I) perchlorate **4-K** (173 mg, 0.13 mmol) in CH_2Cl_2 (20 mL) and stirred for 16 h at r.t. Then, solid Pd(OAc)₂ (87 mg, 0.39 mmol) was added, and the reaction mixture was stirred for 4 h. The solvent was evaporated under reduced pressure, and the residue was dissolved in CH_2Cl_2 and filtered through a column (SiO_2 ; CH_2Cl_2 /MeOH, 98:2). The crude material was purified by GPC (CHCl_3) to afford **6-2H**· 2ClO_4 as a red-orange solid (58 mg, 20%). Selected data for **5-H**· ClO_4 : IR (KBr): $\tilde{\nu}$ = 1100 (ClO_4^-) cm^{-1} . MS (FAB): m/z (%) = 1715 (18) [$\text{M} - \text{ClO}_4$] $^+$. Selected data for **6-2H**· 2ClO_4 : M.p. 184–187 °C. ^1H NMR (400 MHz, $[\text{D}_6]\text{DMSO}$, 25 °C): δ = 9.22 (s, 2 H, *j'*), 9.06 (m, 4 H, *D*), 8.68 (s, 2 H, *j*), 8.33 (m, 2 H, *m*), 8.32 (s, 2 H, *k*), 8.03 (m, 2 H, *l*), 7.36 (m, 4 H, *i*), 7.25 (m, 8 H, *C*), 7.11 (m, 8 H, *B*), 6.95 (m, 4 H, *b*), 6.83 (m, 8 H, *g, a*), 6.75 (t, J = 8 Hz, 2 H, *h*), 6.47 (br., 2 H, *h'*), 4.79 (br., 8 H, *A*), 4.22 (m, 8 H, *c*), 4.12 (m, 4 H, *e*), 4.02 (m, 4 H, *e'*), 3.91 (br., 8 H, *d*), 3.81 (br., 8 H, *f*) ppm. IR (KBr): $\tilde{\nu}$ = 3181, 2060, 1856, 1525, 1488, 1382, 1090 (ClO_4^-), 989, 687 cm^{-1} . MS (FAB): m/z (%) = 2023 (6) [$\text{M} - 1 - \text{ClO}_4$] $^+$, 1012 (13) [$\text{M} - 2\text{ClO}_4$] $^{2+}$.

8-H· $\text{Rh}(\text{TPP})\text{Cl} \cdot \text{ClO}_4$: The thread-like salt **7-H**· O_2CCF_3 (44 mg, 0.12 mmol) was added to a CH_2Cl_2 /MeCN (10:1, 50 mL) solution of the salophen macrocycle with palladium(II)–sodium(I) **1b**· $\text{Pd}^{\text{II}}\text{-Na}(\text{I})$ (100 mg, 0.12 mmol) and stirred for 1 h at r.t. Then, solid $\text{Rh}(\text{TPP})\text{Cl}$ (90 mg, 0.12 mmol) was added, and the reaction mixture was stirred for 60 h. The solvent was evaporated under reduced pressure. The residue was dissolved in CH_2Cl_2 and chromatographed (SiO_2 ; CH_2Cl_2 /MeOH, 98:2) to afford the **8-H**· $\text{Rh}(\text{TPP})\text{Cl} \cdot \text{ClO}_4$ as a violet solid (86 mg, 40%). ^1H NMR (400 MHz, CDCl_3 , 25 °C): δ = 8.79 (s, 10 H, *j, g*), 8.35 (br., 2 H, *H*), 8.24 (m, 4 H, *5*), 8.04 (m, 2 H, *F*), 7.83 (d, J = 7 Hz, 4 H, *4*), 7.70 (m, 8 H, *1, 3*), 7.52 (m, 4 H, *2*), 7.33 (m, 2 H, *k*), 7.11 (br., 2 H, *E*), 6.85 (m, 2 H, *b*), 6.70 (d, J = 8 Hz, 2 H, *g*), 6.65 (m, 2 H, *a*), 6.53 (d, J = 8 Hz, 2 H, *l*), 6.33 (m, 2 H, *i*), 6.17 (m, 2 H, *h*), 5.44 (m, 2 H, *B*), 4.13 (m, 4 H, *c*), 4.01 (m, 8 H, *f, e*), 3.95 (m, 4 H, *d*), 3.84 (m, 2 H, *C*), 3.75 (br., 2 H, *D*), 1.05 (d, J = 7 Hz, 2 H, *A*), 0.88 (s, 9 H, *G*) ppm. MS (MALDI-TOF): m/z (%) = 835 (4) [$\text{M} - 1 - \text{ClO}_4 - \text{Cl}$] $^{2+}$.

X-ray Measurements: X-ray data were obtained with a Bruker SMART-CCD diffractometer; structural determination and refinement were performed by using SAINT^[18] and SHELXTL^[19] software packages, and the empirical absorption correction was performed by using the SADABS^[20] program. All structures were solved by direct methods and refined by a full-matrix least-squares method.

Crystallographic Data

3a-H· PF_6 : $[\text{Ni}(\text{C}_{30}\text{H}_{32}\text{N}_2\text{O}_8)\text{C}_{22}\text{H}_{32}\text{N}_2]_2(\text{PF}_6)_2 \cdot \text{CH}_2\text{Cl}_2 \cdot \text{C}_4\text{H}_8\text{O}_2$, $\text{C}_{109}\text{H}_{138}\text{Cl}_2\text{F}_{12}\text{N}_6\text{Ni}_2\text{O}_{18}\text{P}_2$, M = 2298.51, monoclinic, space group $C2/c$, a = 67.469(4) Å, b = 13.7577(8) Å, c = 24.5387(14) Å, β = 96.183(2)°, V = 22645(2) Å³, Z = 8, ρ_{calcd} = 1.348 g cm^{-3} , $\mu(\text{Mo-K}\alpha)$ = 4.94 cm^{-1} , T = 183(2) K, yellow-brown plates, $0.20 \times 0.15 \times 0.10$ mm, R_1 = 0.0819 [$I > 2\sigma(I)$], wR_2 = 0.2822 (all data), GOF = 0.940.

3b-H-PF₆: [Ni(C₃₄H₃₂N₂O₈)C₂₂H₃₂N]PF₆, C₅₆H₆₄F₆N₃NiO₈P, *M* = 1110.78, triclinic, space group *P* $\bar{1}$, *a* = 11.8973(12) Å, *b* = 15.3612(16) Å, *c* = 15.4538(16) Å, α = 104.457(2)°, β = 97.949(2)°, γ = 96.015(2)°, *V* = 2679.8(5) Å³, *Z* = 2, $\rho_{\text{calcd.}}$ = 1.377 g cm⁻³, $\mu(\text{Mo-K}\alpha)$ = 4.70 cm⁻¹, *T* = 203(2) K, dark-brown plates, 0.40 × 0.30 × 0.20 mm, *R*₁ = 0.0538 [*I* > 2σ(*I*)], *wR*₂ = 0.1645 (all data), GOF = 1.055. **4-Ba**: [Ba₂(C₆₈H₆₆N₄O₁₆)(ClO₄)(MeOH)₃(H₂O)₂](ClO₄)₃(H₂O)₃, C₇₁H₈₈Ba₂Cl₄N₄O₄₀, *M* = 2053.93, triclinic, space group *P* $\bar{1}$, *a* = 10.4086(9) Å, *b* = 18.7294(16) Å, *c* = 23.9428(20) Å, α = 107.823(2)°, β = 99.645(2)°, γ = 91.602(2)°, *V* = 4365.1(6) Å³, *Z* = 2, $\rho_{\text{calcd.}}$ = 1.563 g cm⁻³, $\mu(\text{Mo-K}\alpha)$ = 11.12 cm⁻¹, *T* = 183 K, orange plates, 0.35 × 0.20 × 0.10 mm, *R*₁ = 0.0812 [*I* > 2σ(*I*)], *wR*₂ = 0.2670 (all data), GOF = 1.060.

CCDC-273373 (for **3a-H-PF₆**), -273372 (for **3b-H-PF₆**), and -622229 (for **4-Ba**) contain the supplementary crystallographic data for this paper. These data can be obtained free of charge from the Cambridge Crystallographic Data Centre via www.ccdc.cam.ac.uk/data_request/cif.

Supporting Information (see also the footnote on the first page of this article): NMR spectroscopic data of **3a/b-H-PF₆** and **8-H-Rh(TPP)ClO₄**, additional crystal structures of **3a/b-H-PF₆** and **4-Ba**, and crystal data for **3a/b-H-PF₆** and **4-Ba**.

Acknowledgments

M. N. thanks the New Energy and Industrial Technology Development Organization (NEDO), Japan, for sponsoring an Industrial Technology Research Grant Program. I. Y. thanks the Japan Society for the Promotion of Science (JSPS) for a postdoctoral fellowship. We thank Dr. P. T. Glink (<http://www.editchem.com>) for valuable discussions.

- [1] a) J.-M. Lehn, *Supramolecular Chemistry: Concepts and Perspectives*, Wiley-VCH, Weinheim, 1995; b) M. Asakawa, P. R. Ashton, V. Balzani, A. Credi, C. Hamers, G. Matternsteig, M. Montalti, A. N. Shipway, N. Spencer, J. F. Stoddart, M. S. Tolley, M. Venturi, A. J. P. White, D. J. Williams, *Angew. Chem. Int. Ed.* **1998**, *37*, 333–337; c) S. I. Jun, J. W. Lee, S. Sakamoto, K. Yamaguchi, K. Kim, *Tetrahedron Lett.* **2000**, *41*, 471–475; d) B. L. Feringa (Ed.), *Molecular Switches*, Wiley-VCH, Weinheim, 2001; e) C. A. Schalley, K. Beizai, F. Vögtle, *Acc. Chem. Res.* **2001**, *34*, 465–476; f) J.-P. Collin, C. Dietrich-Buchecker, P. Gaviña, M. C. Jimenez-Molero, J.-P. Sauvage, *Acc. Chem. Res.* **2001**, *34*, 477–487; g) V. Balzani, M. Venturi, A. Credi, *Molecular Devices and Machines*, Wiley-VCH, Weinheim, 2003; h) D. A. Leigh, J. K. Y. Wong, F. Dehez, F. Zerbetto, *Nature* **2003**, *424*, 174–179; i) R. Hernandez, H.-R. Tseng, J. W. Wong, J. F. Stoddart, J. I. Zink, *J. Am. Chem. Soc.* **2004**, *126*, 3370–3371; j) J. D. Badjić, V. Balzani, A. Credi, S. Silvi, J. F. Stoddart, *Science* **2004**, *303*, 1845–1849.
- [2] a) P. T. Glink, A. I. Oliva, J. F. Stoddart, A. J. P. White, D. J. Williams, *Angew. Chem. Int. Ed.* **2001**, *40*, 1870–1875; b) F. G. Gatti, D. A. Leigh, S. A. Nepogodiev, A. M. Z. Slawin, S. J. Teat, J. K. Y. Wong, *J. Am. Chem. Soc.* **2001**, *123*, 5983–5989; c) M. Asakawa, G. Brancato, M. Fanti, D. A. Leigh, T. Shimizu, A. M. Z. Slawin, J. K. Y. Wong, F. Zerbetto, S. J. Zhang, *J. Am. Chem. Soc.* **2002**, *124*, 2939–2950; d) J. A. Wisner, P. D. Beer, M. G. B. Drew, M. R. Sambrook, *J. Am. Chem. Soc.* **2002**, *124*, 12469–12476.
- [3] a) S. J. Cantrill, D. A. Fulton, M. C. T. Fyfe, J. F. Stoddart, A. J. P. White, D. J. Williams, *Tetrahedron Lett.* **1999**, *40*, 3669–3672; b) J. Cao, M. C. T. Fyfe, J. F. Stoddart, G. R. L. Cousins, P. T. Glink, *J. Org. Chem.* **2000**, *65*, 1937–1946; c) Y. Tachibana, N. Kihara, Y. Ohga, T. Takata, *Chem. Lett.* **2000**, 806–807; d) S. J. Cantrill, D. A. Fulton, A. M. Heiss, A. R. Pease, J. F. Stoddart, A. J. P. White, D. J. Williams, *Chem. Eur. J.* **2000**, *6*, 2274–2287.
- [4] a) M. Händel, M. Plevoets, S. Gestermann, F. Vögtle, *Angew. Chem. Int. Ed. Engl.* **1997**, *36*, 1199–1201; b) P. R. Ashton, M. C. T. Fyfe, C. Schiavo, J. F. Stoddart, A. J. P. White, D. J. Williams, *Tetrahedron Lett.* **1998**, *39*, 5455–5458; c) P. R. Ashton, I. Baxter, M. C. T. Fyfe, F. M. Raymo, N. Spencer, J. F. Stoddart, A. J. P. White, D. J. Williams, *J. Am. Chem. Soc.* **1998**, *120*, 2297–2307; d) S. J. Cantrill, J. A. Preece, J. F. Stoddart, Z.-H. Wang, A. J. P. White, D. J. Williams, *Tetrahedron* **2000**, *56*, 6675–6681.
- [5] a) M. Asakawa, M. Higuchi, G. Matternsteig, T. Nakamura, A. R. Pease, F. M. Raymo, T. Shimizu, J. F. Stoddart, *Adv. Mater.* **2000**, *12*, 1099–1102; b) C. D. Nadai, C. M. Whelan, C. Perollier, G. Clarkson, D. A. Leigh, R. Caudano, P. Rudolf, *Surf. Sci.* **2000**, *454*, 112–117.
- [6] a) M. Asakawa, T. Ikeda, N. Yui, T. Shimizu, *Chem. Lett.* **2002**, 174–175; b) T. Ikeda, M. Asakawa, M. Goto, Y. Nagawa, T. Shimizu, *Eur. J. Org. Chem.* **2003**, 3744–3751; c) T. Ikeda, M. Asakawa, M. Goto, K. Miyake, T. Ishida, T. Shimizu, *Langmuir* **2004**, *20*, 5454–5459; d) T. Ikeda, M. Asakawa, T. Shimizu, *New J. Chem.* **2004**, *28*, 870–873; e) T. Ikeda, M. Asakawa, K. Miyake, T. Shimizu, *Chem. Lett.* **2004**, *33*, 1418–1419; f) J. Otsuki, S. Kawaguchi, T. Yamakawa, M. Asakawa, K. Miyake, *Langmuir* **2006**, *22*, 5708–5715.
- [7] a) M. C. Jiménez, C. Dietrich-Buchecker, J.-P. Sauvage, A. D. Cian, *Angew. Chem. Int. Ed.* **2000**, *39*, 1295–1298; b) M. Linke, J.-C. Chambron, V. Heitz, J.-P. Sauvage, S. Encinas, F. Barigelletti, L. Flamigni, *J. Am. Chem. Soc.* **2000**, *122*, 11834–11844; c) J.-P. Sauvage, *Science* **2001**, *291*, 2105–2106; d) M. Andersson, M. Linke, J.-C. Chambron, J. Davidsson, V. Heitz, L. Hammarström, J.-P. Sauvage, *J. Am. Chem. Soc.* **2002**, *124*, 4347–4362; e) C. Dietrich-Buchecker, B. Colasson, M. Fujita, A. Hori, N. Geum, S. Sakamoto, K. Yamaguchi, J.-P. Sauvage, *J. Am. Chem. Soc.* **2003**, *125*, 5717–5725; f) P. Mobian, J.-M. Kern, J.-P. Sauvage, *Angew. Chem. Int. Ed.* **2004**, *43*, 2392–2395.
- [8] I. Yoon, M. Narita, T. Shimizu, M. Asakawa, *J. Am. Chem. Soc.* **2004**, *126*, 16740–16741.
- [9] I. Yoon, M. Narita, M. Goto, T. Shimizu, M. Asakawa, *Org. Lett.* **2006**, *8*, 2341–2344.
- [10] a) T. Katsuki, *Coord. Chem. Rev.* **1995**, *140*, 189–214; b) J. Wöltinger, J.-E. Bäckvall, Á. Zsigmond, *Chem. Eur. J.* **1999**, *5*, 1460–1467; c) V. v. A. Castelli, A. D. Cort, L. Mandolini, D. N. Reinhoudt, L. Schiaffino, *Eur. J. Org. Chem.* **2003**, 627–633.
- [11] a) S. D. Bella, I. Fragalà, I. Ledoux, M. A. Diaz-Garcia, P. G. Lacroix, T. J. Marks, *Chem. Mater.* **1994**, *6*, 881–883; b) P. G. Lacroix, S. D. Bella, I. Ledoux, *Chem. Mater.* **1996**, *8*, 541–545; c) H.-C. Zhang, W.-S. Huang, L. Pu, *J. Org. Chem.* **2001**, *66*, 481–487.
- [12] a) R. Foster, *Organic Charge Transfer Complexes*, Academic, London, 1969; b) F. Franceschi, E. Solari, C. Floriani, M. Rosi, A. Chiesi-Villa, C. Rizzoli, *Chem. Eur. J.* **1999**, *5*, 708–721; c) F. Franceschi, E. Solari, R. Scopelliti, C. Floriani, *Angew. Chem. Int. Ed.* **2000**, *39*, 1685–1687; d) I. Yoon, M. Goto, T. Shimizu, S. S. Lee, M. Asakawa, *Dalton Trans.* **2004**, 1513–1515.
- [13] M. Asakawa, T. Shimizu, manuscript in preparation.
- [14] a) G. R. Desiraju, *Acc. Chem. Res.* **1991**, *24*, 290–296; b) F. M. Raymo, M. D. Bartberger, K. N. Houk, J. F. Stoddart, *J. Am. Chem. Soc.* **2001**, *123*, 9264–9267; c) T. Steiner, *Angew. Chem. Int. Ed.* **2002**, *41*, 48–76.
- [15] a) C. A. Hunter, J. K. M. Sanders, *J. Am. Chem. Soc.* **1990**, *112*, 5525–5534; b) H. Adams, C. A. Hunter, K. R. Lawson, J. Perkins, S. E. Spey, C. J. Urch, J. M. Sanderson, *Chem. Eur. J.* **2001**, *7*, 4863–4877.
- [16] H. Ogoshi, J. Setsumo, T. Omura, Z. Yoshida, *J. Am. Chem. Soc.* **1975**, *97*, 6461–6466.
- [17] a) P. R. Ashton, P. T. Glink, J. F. Stoddart, S. Menzer, P. A. Tasker, A. J. P. White, D. J. Williams, *Tetrahedron Lett.* **1996**,

- 37, 6217–6220; b) P. R. Ashton, R. Ballardini, V. Balzani, M. Gómez-López, S. E. Lawrence, M. V. Martínez-Díaz, M. Montalti, A. Piersanti, L. Prodi, J. F. Stoddart, D. J. Williams, *J. Am. Chem. Soc.* **1997**, *119*, 10641–10651; c) S. J. Cantrill, M. C. T. Fyfe, A. M. Heiss, J. F. Stoddart, A. J. P. White, D. J. Williams, *Chem. Commun.* **1999**, 1251–1252; d) S. J. Cantrill, M. C. T. Fyfe, A. M. Heiss, J. F. Stoddart, A. J. P. White, D. J. Williams, *Org. Lett.* **2000**, *2*, 61–64.
- [18] *SAINTPLUS Version 6.22*, Bruker AXS, Madison, WI, USA.
[19] G. M. Sheldrick, *SHELXTL Version 6.12*, Bruker AXS, Madison, WI, USA, **2000**.
[20] G. M. Sheldrick, *SADABS: Program for Scaling and Correction of Area Detector Data*, University of Göttingen, Germany, **1998**.

Received: February 14, 2007
Published Online: July 18, 2007